# Statistical Properties of the Forced Lorentz Chaos : Synergetic Approach to the System Identification (Random Systems and Dynamical Systems)

AUTHOR(S):

AIZAWA, YOJI

数理解析研究所講究録
439巻 1981年 63-88



# Statistical Properties of the forced Lorenz Chaos
## — Synergetic Approach to the System Identification —

Yoji AIZAWA

Department of Physics, Kyoto University, Kyoto, Japan

synopsis

The forced Lorenz System is studied synergetically with the main regard to the statistical identification of the non-periodic motion. The following points are reported;

1. Phase diagram of the entrainment
2. Spectral density and time correlation function
3. Recurrence time distribution
4. Lyapounov spectrum
5. Theoretical reconstruction of the time correlation function
6. Hausdorff dimension of the symbolic time series
7. Hausdorff dimension of the strange attractor
8. Intermittency
9. Supplementary discussion

§1. phase diagram

The following non-antonomous system is considered;

$$dx/dt = \sigma(y-x)$$

$$dy/dt = rx-y-xz \qquad (1)$$

$$dz/dt = -bz+xy+A\cos Bt$$

where $\sigma$, r, b, A and B are parameters. When the driving force $A\cos Bt$ is finite, the whole orbits are restricted to a finite volume in phase space as t goes to infinity since the quadratic Lyapounov function is easily found. The symmetry of the system is not diturbed by the external driving force; the system is invariant to the space inversion ($x \to -x$, $y \to -y$ ; $A \to -A$). The original Lorenz chaos is the case of $\sigma = 10$, $r = 28$, $b = 8/3$ and $A = 0$ [2]. When $A \neq 0$, the periodic driving force whose period $T = \frac{B}{2\pi}$, induces the onset of the (partial) coherence through nonlinear internal resonances, and the motion is entrained into an ordered one, which has a higher symmetry than the original Lorenz chaos. The phase diagram of the entrainment is shown in Fig.1. The typical limit cycle motion in each regime is illus-

Fig.1.

trated in Fig.2, those are classified by the alternation of the

Fig.2.

period nT as well as the asymmetry of each orbit. A variety of bifurcations are observed in the neighborhood where the periodic

motion takes the place of nonperiodic one.

## §2. Spectral density S(f) and time correlation function R(t)

S(f) and R(t) are defined as follows,

$$S(f) = \left\langle \frac{1}{NT} \left| \int_0^{NT} y(t) e^{i2\pi ft} dt \right|^2 \right\rangle \qquad (2)$$

and

$$R(t) = \left\langle \frac{1}{NT} \int_0^{NT} y(t') y(t+t') dt' \right\rangle$$

where f stands for the frequency.[3] In the regime for the periodic response, only the line spectra is obtained, but for the non-periodic response S(f) has a continuous component. Figure 3 shows the change of the spectral type for each value of A, where B = 6.0 is fixed. S(f) is shown in Logarithmic plot, and the coordinates x, z and f is in arbitrary unit.

Fig.3.

Increasing the level of the periodic perturbation, the original Lorenz chaos is partially entrained to the modulated internal mode, and as the result,several dominat peaks come to appear in the spectral density function. The long time tail of the time correlation function is closely connected to the onset of the partial coherence. Special attention must be payed to the low frequency domain, where for the case of A = 0 the spectral type is well reproduced by,

$$S(f) \sim f^{-0.5} \qquad (4)$$

## § 3. Recurrence time distribution [4)]

Figure 4 shows the return map of the successive zero-crossing recurrence time $\{T_i\}$ : $x(T_i) = x(T_i + 1) = 0$ . The time course of $x(t)$ (in Fig.5) suggests that the recurrence time is measured by the integral $n_i$ which stands for the number of the oscillation during $T_i$ . The flip-flop jump occurs at the zero crossing time. Therefore, the time course $x(t)$ is represented by the jump process $P(t)$ with discrete time if the coarse-graining projection is applied during each recurrence time. In other words, $x(t)$ is separated into two parts, $P(t)$ and $\theta(t)$ as shown in Fig.5. Figure 6 shows the distribution density $P(m)$ of the

Fig.4, Fig.5

recurrence time $m$ and figure 7 is the distribution density $P(m,N)$ of the flip-flop number $m$ during the time interval $N$ . Both plots in Figs 6 and 7 are adjustable by the exponential distribution and the poissonian distribution respectively, which are shown by the solid lines;

$$P(m) = (1-\bar{m})\ \bar{m}^{m-1} \tag{5}$$

$$P(m,N) = \frac{N!}{m!\,(N-m)!}\ (1-\bar{m})^{N-m}\ \bar{m}^{m} \tag{6}$$

where $\bar{m} = 0.44$ is adopted in both cases. Flip-flop jump process is realized by a $(0,1)$ symbolic time series. Steady distributions are equal for both symbols;

Fig.6, Fig.7

$$P_0 = P_1 = 1/2 \tag{7}$$

and the transition probability is given by,

$$P_{10} = P_{01} = \bar{m} \tag{8}$$

The simple markovian identification mentioned above leads us to the characterization of the nonperiodic flow in terms of the Kolmogorov - Sinai entropy or the Hausdorff dimension which is explained in §5.

## §4. Lyapounov spectrum [5]

The Lyapounov spectra $\{K_i\}$ $(i = 1,2,3)$ are calculated by,

$$\begin{aligned} K_1 &= K_L \\ K_2 &= K_S - K_L \\ K_3 &= K_V - K_S \end{aligned} \tag{9}$$

where $K_V$, $K_S$, and $K_L$ are the stretching rate for the stroboscopic mapping $(f^T : (x_t, y_t, z_t) \to (x_{t+T}, y_{t+T}, z_{t+T}))$ of the volume, surface, and line in the corresponding tangent space, respectively. In the numerical calculation, these values are obtained through averaging over the appropriate ensemble of the initial condition. Figure 8 shows the Lyapounov spectrum for

Fig.8.

each value of $A$. ($B = 6.0$ is fixed.) The estimation error in the averaging calculation is less than 0.02 for each $K_\mu$. The second Lyapounov spectrum $K_2$ is positive for $0 < A \lesssim 21$. Around $A = 21$, however, no considerable singularities have been observed

so far at least in the computer experiments concerning with the adequate poincare map as well as with the time series analysis. On the other hands, around $A = 61$ a kind of structural change is observed in the strange attractor, where the sharp change appears in the third Lyapounov spectrum $K_3$. This situation reminds us of the second order phase transition between two chaotic attractors. It is shown in §6 that the dimension of the strange attractor is an appropriate chaos parameter charactering the chaos-chaos transition.

## §5. Theoretical reconstruction of the time correlation function

As told in §3, $x(t)$ is separated into two parts;

$$x(t) = P(t) + \theta(t) \tag{10}$$

where $P(t)$ is well approximated by the poissonian process. The time correlation function $\Gamma_{(t)} = \langle x(t') \cdot x(t'+t) \rangle$ is given by;

$$\begin{aligned} \Gamma(t) = &\langle P(t')P(t'+t)\rangle + \langle P(t')\theta(t'+t)\rangle \\ &+ \langle \theta(t')P(t'+t)\rangle + \langle \theta(t')\theta(t'+t)\rangle \end{aligned} \tag{11}$$

When $\theta(t)$ is approximated by,

$$\theta(t) = \theta_0 e^{\alpha t}\cos\omega_0 t \quad , \tag{12}$$

$$\theta_c = \theta(T) = \theta_0 e^{\alpha t}\cos\omega_0 T$$

where, $\theta_c$ is the threshold value above which the flip-flop jump occurs, and $T$ is the zero crossing recurrence time, and $\alpha$, $\omega_0$ are the adjustable parameter for the system under consideration.

The distribution of the initial value $\theta_0$ is given by the recurrence time distribution as follows,

$$P(\theta_0) = \frac{\lambda}{\alpha\theta_0} \left(\frac{\theta c}{\theta_0}\right)^{-\lambda/\alpha} \tag{13}$$

where $\lambda$ characterizes the poissonian process $P(t)$ ;

$$\langle P(t')P(t'+t)\rangle \sim e^{-2\lambda t} \tag{14}$$

Eqs. (11) ~ (14) enable us to derive the analytical expression for $\Gamma(t)$ .

## §6. Hausdorff dimension of the symbolic time series

When the transition probability $P_{01}$ $(= P_{10})$ and the stationary distribution $P_0$ $(= P_1)$ are calculated by the computer experiments, the Hausdorff dimension $D_H$ or the Kolmogorov - Sinai entropy $H_{KS}$ $(= D_H \ln 2)$ is determined [6]

$$D_H = \frac{-1}{\ln 2} \sum_{ij} P_i P_{ij} \ln P_{ij} \tag{15}$$

When $P_{01}$ approaches to zero or unity, the time course of the symbolic dynamics becomes almost invariant or periodic, respectively, and as the result, $D_H$ goes to zero. This situation is called forced intermittency. Increasing the level of the external regular perturbation, it seems that the forced intermittent chaos comes to appear. Figure 9 shows the Hausdorff dimension

Fig.9.

for the forced Lorenz chaos. The Hausdorff dimension decreases monotonically for $0 < A < 20$ . $(D_H(A = 0) = 0.9895)$. As for $A > 15$ ,

the simple markovian identification breaks down partially, it is difficult to certify the appearence of the forced intermittency in the present system. The problems of the intermittency is lightened again from the another angle in § 8, where the free intermittent chaos is discussed carrying out with the autonomous Lorenz system.

## §7. Hausdorff dimension of the strange attractor[6),7)]

The outer measure $\ell(\alpha)$ is calculated by the computer simulation as follows,[6)]

$$\ell(\alpha) = \inf \sum_i (\mathrm{diam} S_i)^\alpha \simeq \rho^\alpha N \tag{16}$$

where,

$$\rho = \mathrm{diam} S_i \simeq \frac{|df^T(e_1 \wedge e_2 \wedge e_3)|}{|df^T(e_1 \wedge e_2)|}$$

$$N = \rho^{-3} |df^T(e_1 \wedge e_2 \wedge e_3)| \tag{17}$$

Here, $df^T$ is the T-time shift operator in the tangent space and $e_i$ is the unit eigen vector corresponding to the Lyapounov No.$K_i$. Using the numerical approximate form of eq.(17),

$$\ell(\alpha) = \exp\{T\ \{K_3(\alpha-3)+\Sigma K_i\}\} \tag{18}$$

Therefore, the Hausdorff dimension of the strange attractor $D_A$ is estimated at the change over point of $\ell(\alpha)$ for $T \to \infty$ as follows,

$$D_A = 3 - \frac{\Sigma K_i}{K_3} \tag{19}$$

which is shown in Fig.10. Except the point of $A \cong 61$ where

Fig.10.

singularity is observed, $D_A$ seems a smooth function of $A$. ($D_{A=0} = 2.06$). For $83 \lesssim A \lesssim 116$, the motion is periodic.

In the projected k-dimensional space spaned by $\{e_{i_1}, e_{i_2}, \ldots e_{i_k}\}$, in general, the dimension spectrum $D_A(i_1,\ldots i_k)$ is given by,

$$D_A(i_1,i_2,\ldots;i_k) = k - \frac{\sum_K K_{i_K}}{K_k} \tag{20}$$

Here the diameter $\rho$ and the number of the covering $N$ are defined as follows,

$$\rho = \frac{|df^T(e_1 \wedge e_2 \wedge \ldots \wedge e_k)|}{|df^T(e_1 \wedge e_2 \wedge \ldots \wedge e_{k-1})|}$$
$$N = \rho^{-k}|df^T(e_1 \wedge e_2 \wedge \ldots \wedge e_k)| \tag{21}$$

and $K_1 \geq K_2 \geq \ldots \geq K_k$, $K_k \neq 0$ are assumed. The dimension spectrum is negative when the mapping is expanding in the projected space. If the computational argorithm of the outer measure is refined taking the curvature of the flow into account, it may be possible to get the much more precise estimation of the dimension of the strange attractor.

## §8. Intermittency [8]

In what follows, discussion is limitted to the autonomous system; $A = 0$. Various types of intermittency are observed in the Lorenz system when the parameters ($r$, $\sigma$, $b$) are taken adequately. Figure 11 shows an example of the intermittency. The

Fig.11.

attractor is a limit cycle for $r \lesssim 166.06$ , where the symbolic time series of the zero-crossing time $\{n_i\}$ is $\{2,2,2, \ldots\}$ . Here $n_i$ stands for the quantized recurrence time as mentioned in §3. For $r > 166.06$ , however, the intermittent chaos comes to appear through destabilization of the limit cycle, where the corresponding symbolic series becomes irregular mixing of $n = 1$ and $n = 2$ . For short that is represented as follows,

$$\{n_i\} = \{2;1\} \tag{22}$$

namely, this means that the uniform series of $\{2\}$ is interrupted intermittently by $n = 1$ . Figure 12 shows the Lorenz plot for

Fig.12, Fig.13, Fig.14

$r = 166.6$. Reducing the value of $r$ , the degree of the interruption decreases and the long range coherence of the symbolic series increases. As shown in Figs. 13 and 14, the level of the continuous spectral component diminishes relatively, and the long time tail appears. For $r \lesssim 166.06$ , the full coherence is attained.

In general, the intermittency in the Lorenz system is represented by the following symbolic series,

$$\{n_i\} = \{m;1,2,\ldots,m-1\} \tag{23}$$

for example, the Lorenz chaos for $(\sigma = 16,\ b = 4,\ r \cong 138)$ is the case of $m = 3$ . If the residence time distribution for $n = m'$ $(\leq m)$ is well approximated by exponential function, it is strongly suggested that the simple markovian identification is possible for the symbolic series $\{n_i\}$ under consideration.

Indeed, the adjustability of the identification was ascertained partially by the computer experiments in the cases mentioned above. This markovian identification enables us to characterize the intermittency in terms of the Hausdorff dimension in the framwork of the markovian assumption as shown in §3.

The intermittency appeared in the Lorenz system is well approximated by the one dimensional $\lambda$ model which is shown in Fig.15; For the case of $D \leq C$, all the motion approaches to a periodic motion but for the case of $D > C$, there appears the chaotic orbit. When the intervals $0 \leq x < A$, and $A \leq x < 1$ are symbolized by 0 and 1, respectively, the recurrence time series satisfies eq.( 23 ).

## § 9. Supplementary discussion

The one-dimensional statistical identification is not always effective for the analysis of the high dimensional chaos or the hyperchaos.[9] In some cases, however, the validity of the one-dimensional identification is recovered by using the appropriate projection or the coarse-graining operation for the state and time. In such circumstances, even the hyterchaos may be understood in the framework of the suitable markovian process in the projected space. At least from the view point of statistical mechanics, it seems that the goal is to find out the projection rule leading to the possible markovian description. The strategic chart used in the present report is summarized in Fig.16.

The time series analysis mentioned in §2 is naturally extented to the high dimensional identification by constructing the corresponding auto-regressive statistical model, where the markovian order of the hyperchaos is reasonablly defined by the computer experiment.[3)]

In § 8 we showed the methodology characteriging the intermittency, where the intermittency degree is measured by the Hausdorff dimension of the corresponding symbolic time series, in other words, by the deviation from the full coherent reference state. Though in § 8 the deviation was well approximated partially by the simple random process, the validity of the markovian identification is not guaranteed in general and that depends strongly on the coarse-graining operation used there. Therefore, from the general view point, it is still an open question whether the intermittency can be described reasonablly in the markovian framework or not.

In §§ 6,7 the dimension spectra defined by eq.(20) were appreciated as the adequate chaos parameters. These are surmised to estimate the approximate value of the self-similarity dimension of the strange attractor from above in each restricted space. It is expected that the formulus is refined more precisely on. Even in the case of the one-dimensional transformation,[10)] many problems remain unsolved as concerns the characterization of the complexity and the randomness of the motion.

References

1) The details of the present report will appear in Prog.Theor.Phys.

2) E.N.Lorenz, J.Atom.Sci.,20 (1963),130
J.L.Kaplan and J.A.Jorke, Commun.Math.Phys.67 (1977),93
I.Shimada, Prog.Theor.Phys.,62 (1979),61
V.Franceschini, J.Stat.Phys.,22 (1980),397

3) E.O.Brigham,'The fast fourier transform',(Prentice-Hall Inc, New York,1974)
H.Akaike, Ann.Inst.Statist.Math.22 (1970),203,219

4) T.T.Soong,'Random differential equation in science and engineering',(Acad.Press,New York,1973)

5) A.G.Kusnirenko, Sov.Math.Dokl.,161 (1965),360
V.I.Oseledec, Trans.Moscow Math.Soc.,19 (1968),197
Ja.B.Pesin, Sov.Math.Dokl.,17 (1976),196

6) P.Billingsley,'Ergodic theory and Information',(John-Wiley & Sons,New York,1960)

7) B.B.Mandelbrott,'Fractals:form,cnance and dimension', (W.H.Freeman and Campany,1977)
D.Ruelle,'Thermodynamic formalism', (Addison-Wesley Publishing, 1978), chapter 7
H.Mori and H.Fujisaka, Prog.Theor.Phys. 63 (1980),1931

8) P.Manneville & Y.Pomeau, Phys.Letts.75A (1979),1
P.Manneville, J.de Physique, (1980)
A.A.Townsend,'The structure of turbulent shear flow', (Cambridge Univ.Press,London,1976)
C.Dopazo & E.E.O'Brien,'Turbulent shear flows I', eds.F.Durst et al,(Springer, 1979),6

J.O.Hinze,'Turbulence',(McGraw-Hill,1975)

V.Frisch,P.L.Sulem and M.A.Nelkin, J.Fluid Mech. 87(1978),719

9) O.E.Rössler,'Synergetics',ed.H.Haken,(Springer,1979),290

R.H.G.Helleman,'Fundamental Problems in Statistical Mechanics',ed.E.G.D.Cohen,(North Holland Publ.,Amsterdam and New York,1980),165

10) Y.Takahashi,Osaka J.Math. 10 (1973),175

Sh.Ito,H.Nakano and S.Tanaka,Tokyo J.Math. 2 (1979)222,241

S.Grossman and S.Thomae, Z.Naturforsch., 329 (1977),1353

R.M.Mays and G.Oster, Amer.Naturalist 110 (1976),573

M.J.Feigenbaum, J.Stat.Phys. 21 (1979),669

J.Guckenheimer, Comm.Math.Phys. 70 (1979),133

N.Metropolis,M.L.Stein and P.R.Stein, J.Ccombinatorial Theory 15 (1973),25

## Figure Captions

Fig.1. Phase diagram of entrainment.
($r = 28$, $\sigma = 10$, $b = 8/3$) Chaotic response appears in the dark region and periodic one in the white region.

Fig.2. Magnification of phase diagram
Typical periodic orbit is illustrated in x - z plane.

Fig.3. Orbit, power spectral density and time corelation function.
($r = 28$, $\sigma = 10$, $b = 8/3$)

Fig.4. Return map of the zero-crossing time
($r = 28$, $\sigma = 10$, $b = 8/3$, $A = 0$)

Fig.5. Time course of $x(t)$ and Flip-Flip jump process
($r = 28$, $\sigma = 10$, $b = 8/3$, $A = 0$)

Fig.6. Number distribution of the flip-flop jump event
($r = 28$, $\sigma = 10$, $b = 8/3$, $A = 0$)

Fig.7. Recurrence time distribution
($r = 28$, $\sigma = 10$, $b = 8/3$, $A = 0$)

Fig.8. Lyapounov spectra
($r = 28$, $\sigma = 10$, $b = 8/3$, $B = 6.0$)

Fig.9. Hausdorff dimension of the symbolic time series.
($r = 28$, $\sigma = 10$, $b = 8/3$, $B = 6.0$)

Fig.10. Hausdorff dimension of the strange attractor.
($r = 28$, $\sigma = 10$, $b = 8/3$, $B = 6.0$)

Fig.11. First Lyapounov spectrum for the intermittent chaos.
($\sigma = 10$, $b = 8/3$, $A = 0$)

Fig.12. Lorenz plot for the intermittent chaos.
($\sigma = 10$, $b = 8/3$, $r = 166.6$, $A = 0$)

Fig.13. Spectral evolution of the intermittent chaos.
a) $\sigma = 10$, $b = 8/3$, $r = 166.6$, $A = 0$
b) $\sigma = 10$, $b = 8/3$, $r = 166.13$, $A = 0$

Fig.14. Onset of the long range coherence in the intermittent chaos.
a) $\sigma = 10$, $b = 8/3$, $r = 166.6$, $A = 0$
b) $\sigma = 10$, $b = 8/3$, $r = 166.1$, $A = 0$

Fig.15. One-dimensional $\lambda$ model for the intermittent chaos.
a) $\sigma = 16$, $b = 4$, $r \cong 138.0$, $A = 0$
b) $\sigma = 10$, $b = 8/3$, $r \cong 166.1$, $A = 0$

Fig.16. Strategic flow chart.

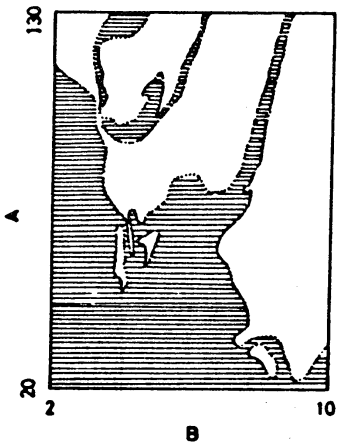


Fig.1

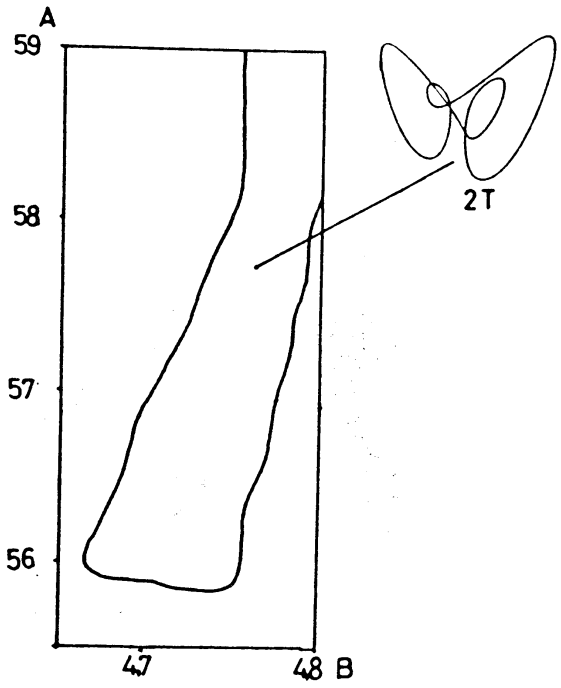


Fig.2-(a)

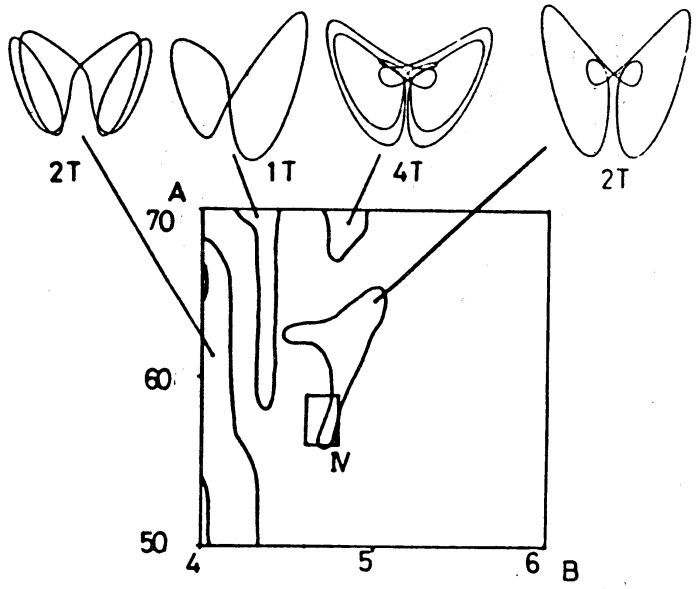


Fig.2-(b)

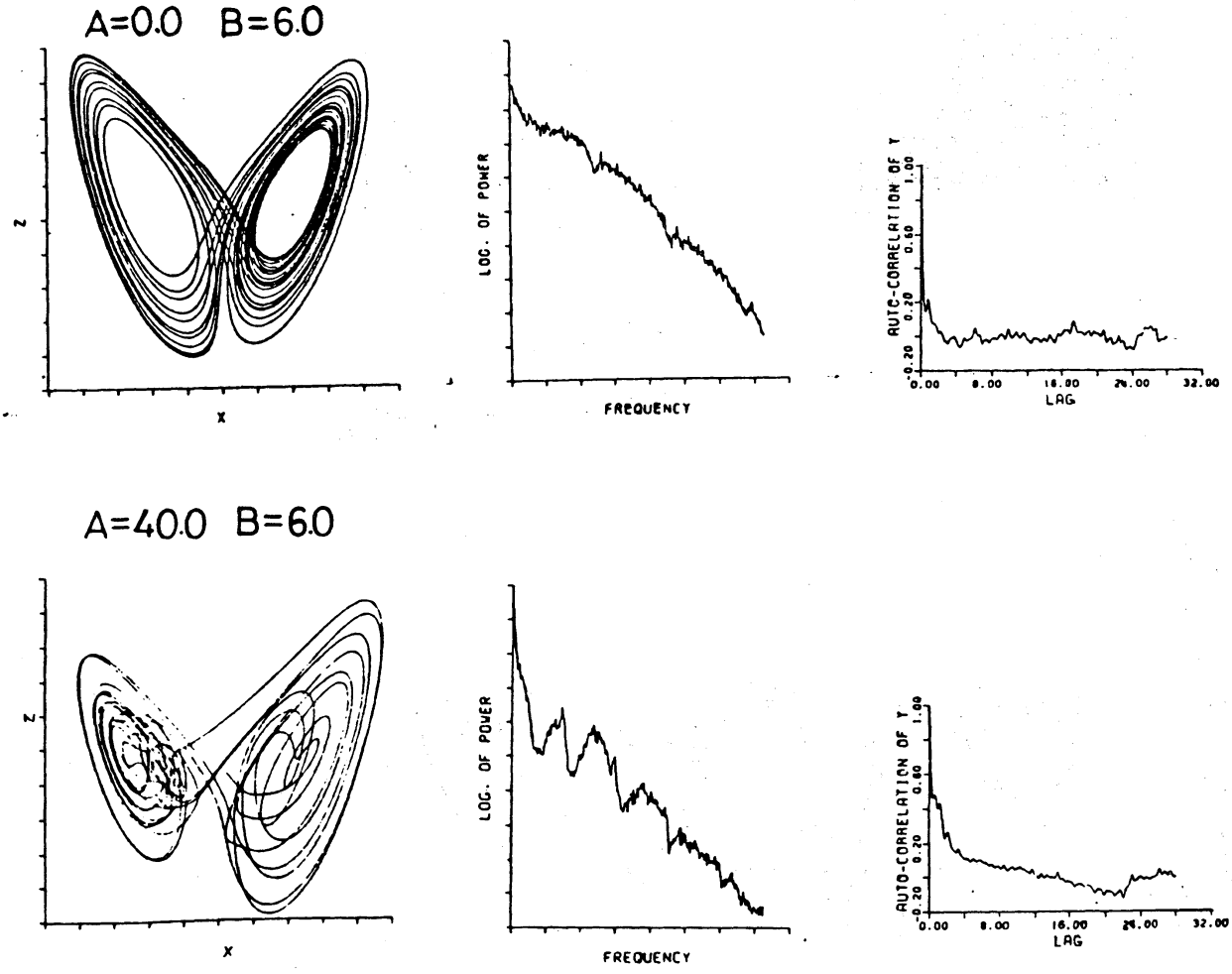
A=0.0 B=6.0
Z
X
LOG. OF POWER
FREQUENCY
AUTO-CORRELATION OF Y
1.00
0.60
0.20
-0.20
0.00
8.00
16.00
24.00
32.00
LAG
A=40.0 B=6.0
Z
X
LOG. OF POWER
FREQUENCY
AUTO-CORRELATION OF Y
1.00
0.60
0.20
-0.20
0.00
8.00
16.00
24.00
32.00
LAG

Fig.3-(a)

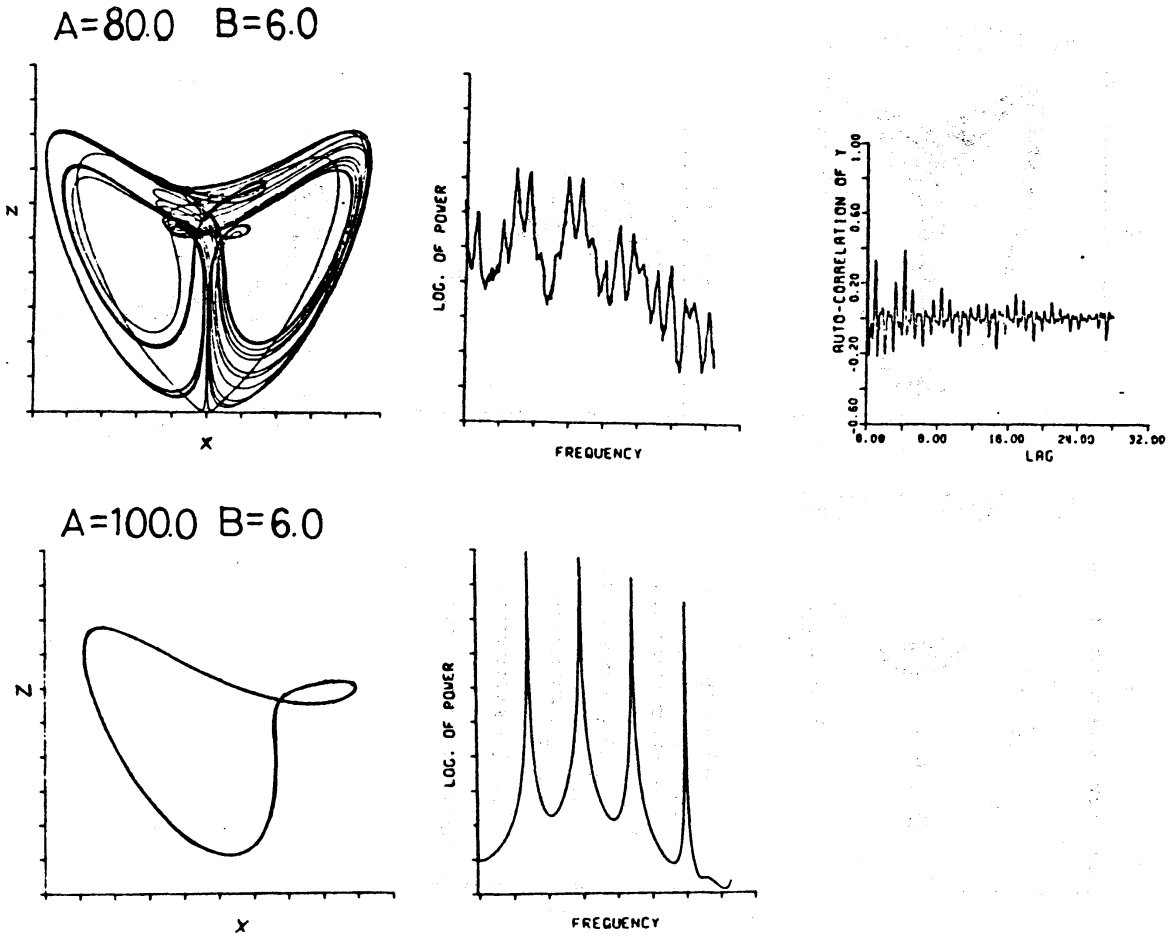
A=80.0 B=6.0
Z
X
LOG. OF POWER
FREQUENCY
AUTO-CORRELATION OF Y
1.00
0.60
0.20
-0.20
-0.60
0.00
8.00
16.00
24.00
32.00
LAG
A=100.0 B=6.0
Z
X
LOG. OF POWER
FREQUENCY

Fig.3-(b)

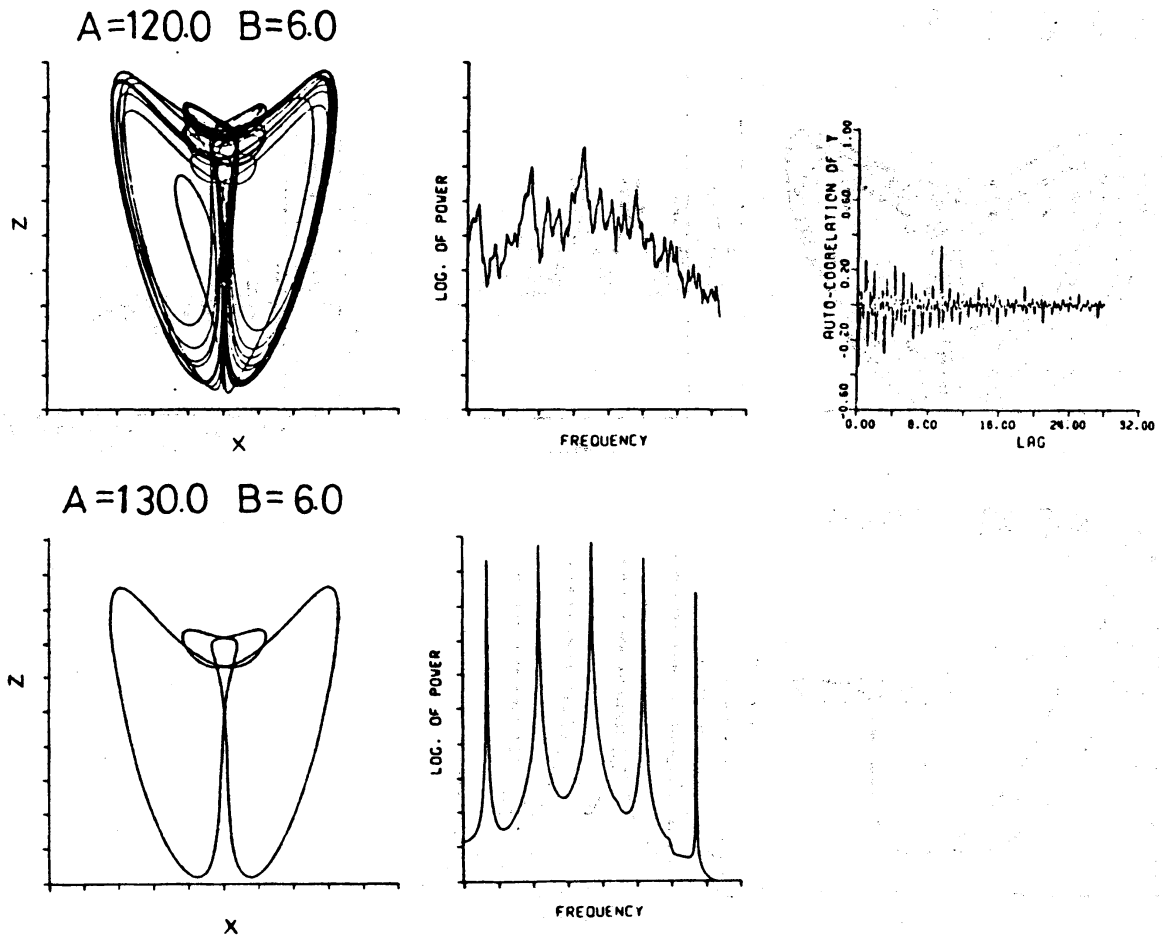
A=120.0 B=6.0
Z
X
LOG. OF POWER
FREQUENCY
AUTO-CORRELATION OF Y
1.00
0.60
0.20
-0.20
-0.60
0.00
8.00
16.00
24.00
32.00
LAG
A=130.0 B=6.0
Z
X
LOG. OF POWER
FREQUENCY

Fig.3-(c)

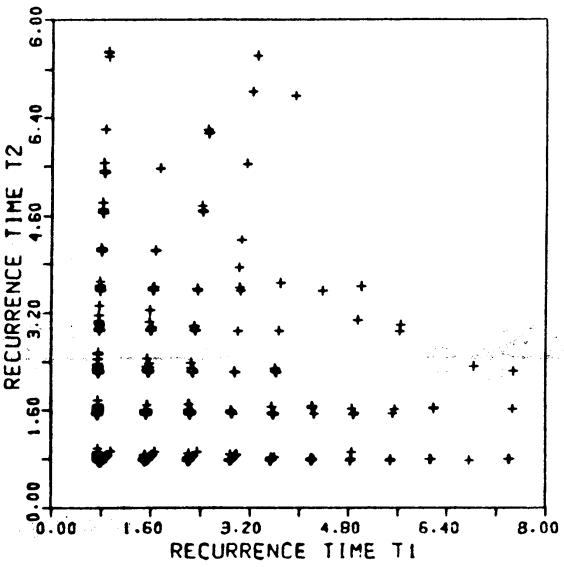
RECURRENCE TIME T2
0.00
1.60
3.20
4.80
6.40
8.00
RECURRENCE TIME T1

Fig.4

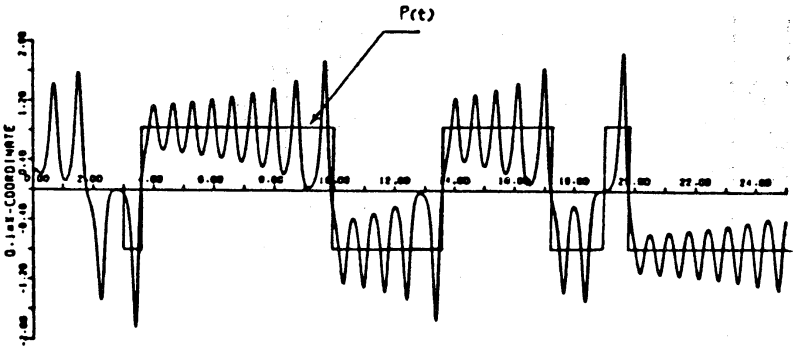
P(t)

Fig.5

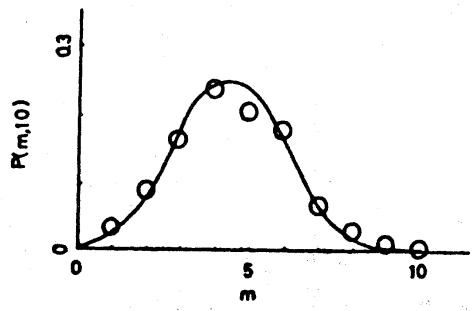


Fig.6

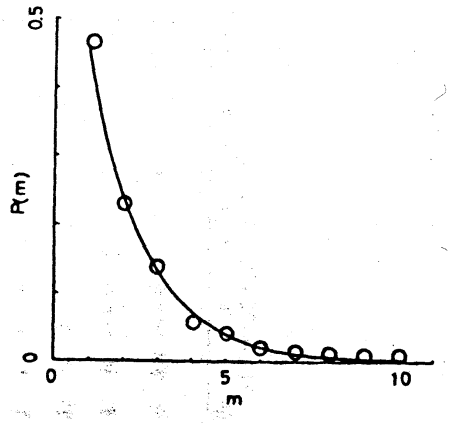


Fig.7

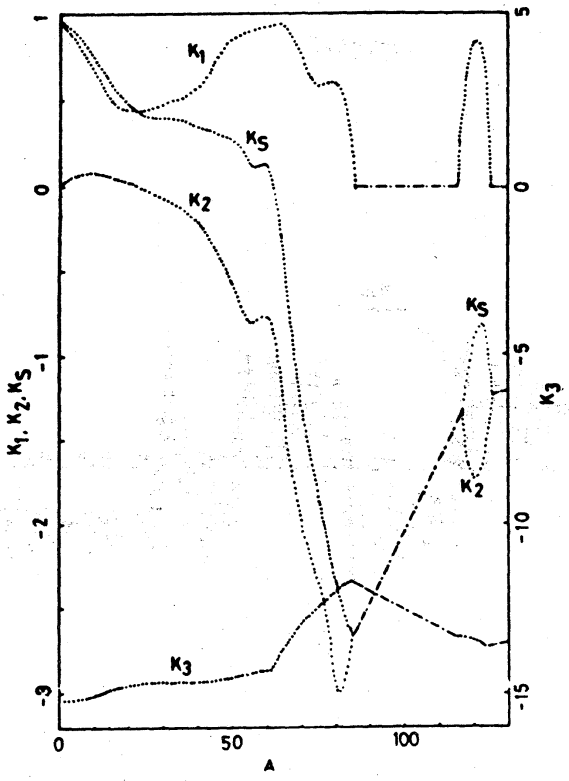


Fig.8

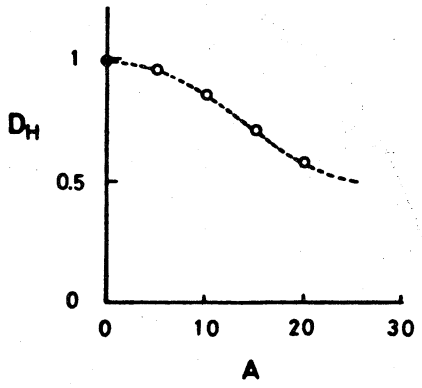


Fig.9

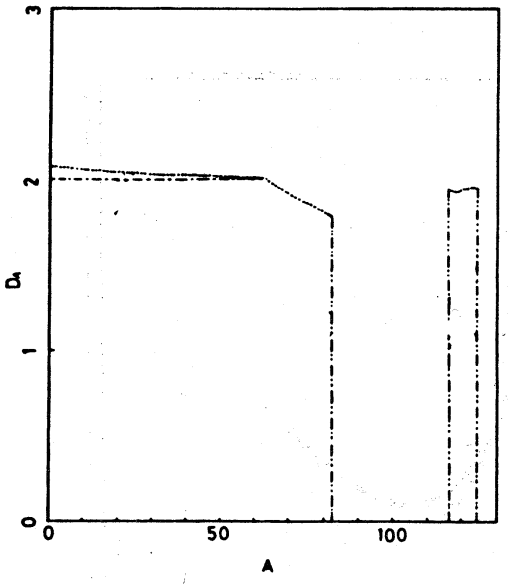


Fig.10

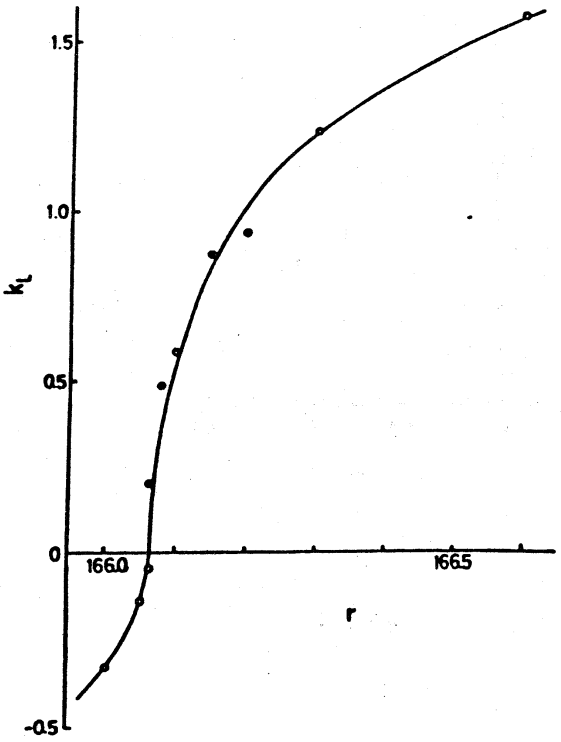


Fig.11

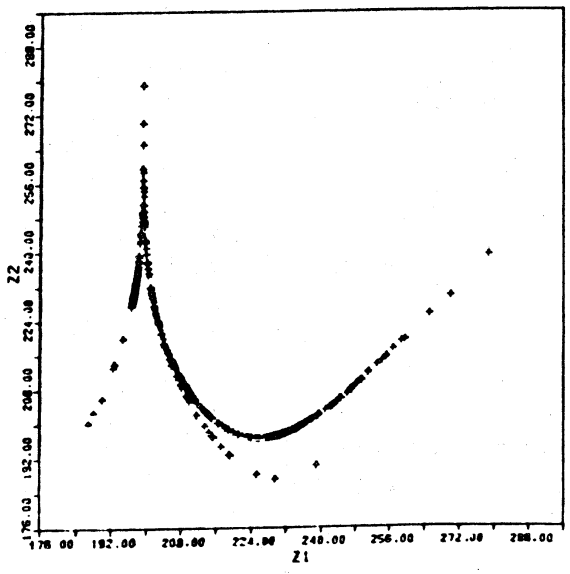


Fig.12

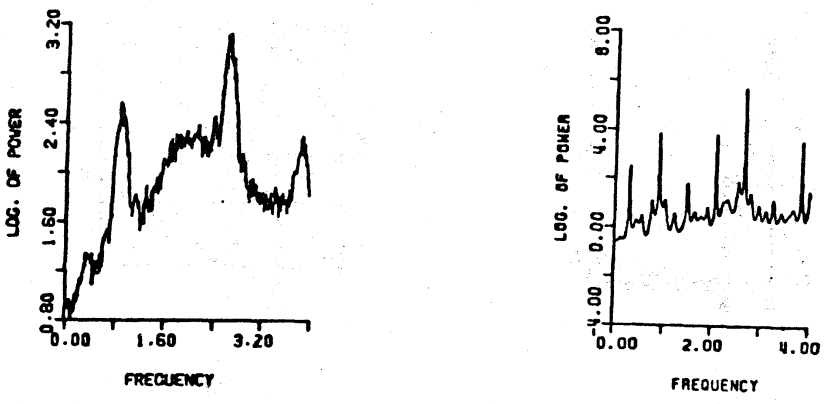


(a) (b)

Fig.13

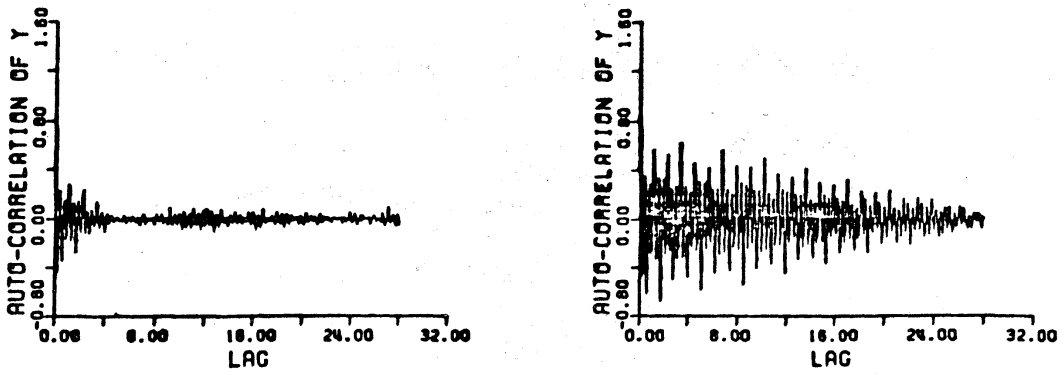


(a) (b)

Fig.14

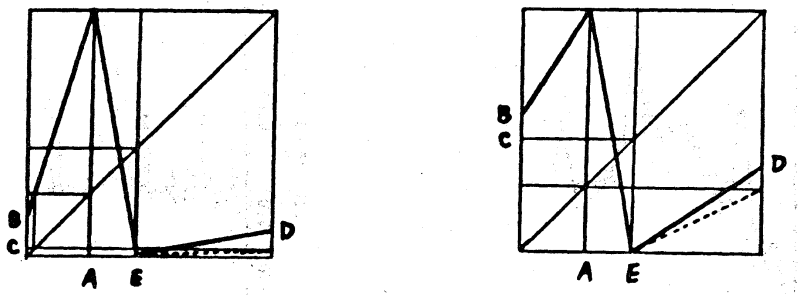
B
C
D
A
E
(a)
B
C
D
A
E
(b)

Fig.15

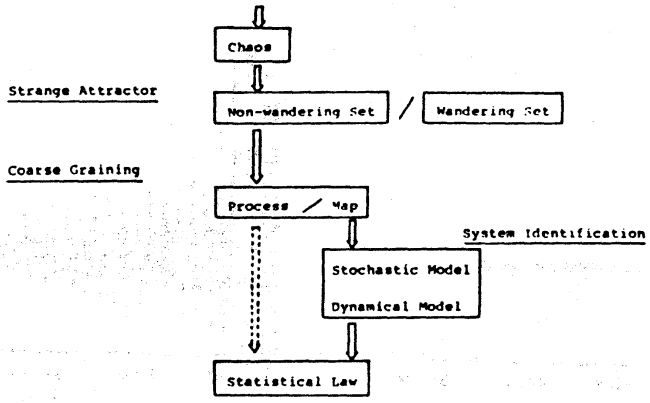
Chaos
Strange Attractor
Non-wandering Set
Wandering Set
Coarse Graining
Process / Map
System Identification
Stochastic Model
Dynamical Model
Statistical Law

Fig.16